A FEATURE BASED CORRESPONDENCE ALGORITHM FOR IMAGE MATCHING

W. Förstner
Institut for Photogrammetry
Stuttgart University

Abstract: A new feature based correspondence algorithm for image matching is presented. The interest operator is optimal for selecting points which promise high matching accuracy, for selecting corners with arbitrary number and orientation of edges or centres of discs, circles or rings. The similarily measure can take the seldomness of the selected points into account. The consistency of the solution is achieved by maximum likelihood type (robust) estimation for the parameters of an object model. Approximate values have to be better than 1/3 of the size of the image in shift, 20 ° in rotation and 30 % in scale.

0. Introduction

The paper describes a new feature based procedure for image matching. It was motivied by the algorithm developped by BARNARD and THOMPSON (1981). Their concept basicly resulted in a three step-procedure. Keeping their motivation for the individual steps, specifically distinctness, similarity and consistency, the steps were replaced by slightly different ones in order to arrive at a procedure with a common theoretical framework, namely a maximum likelihood type estimation for the parallax field (cf. PADERES et. al. 1984). Though the actual implementation uses a comparably simple object model, the concept is general enough to handle piecewise smooth surfaces. The procedure contains a new interest operator, which turned out to have attactive features, as it not only aims at finding points which promise precise parallax determination, but at the same time is an operator to find corners with edges of arbitrary number and orientation as well as the centre of circles, discs or rings. In addition a simple measure of seldomness has been developped in order to increase the reliability of the procedure in presence of repetetive patterns.

Feature based matching (FBM) procedures contrast to gray level or area based methods, like classical image correlation or least squares matching (LSM). FBM is superior to image correlation with respect to speed and versatility and is superior to LSM with respect to range of convergence, speed and versatility. Especially the high requirements for approximate values of LSM, (< 1-2 pixels for shifts, < 20 ° for rotation, < 30 % for scale difference and shear) are reason enough to use different concepts. FBM procedures are widely used in pattern recognition and computer vision (cf. FÖRSTNER 1986) and find increasing interest also in photogrammetry.

We will first outline the basic strategy and the requirements to be met in the individual steps, and give an example. Section 2 then describes the maximum likelihood type estimation of the parameters of the mapping function between the images. The determination of preliminary weights for this robust estimation are discussed in section 3. It is based on the points selected by the new interest operator whose properties are described in detail in section 4.

1. Concept of Feature Based Matching

FBM procedures consist of three steps:

1. selecting distinct points in the images separately using a socalled interest operator.
2. building up a preliminary list of candidate pairs of corresponding points assuming a similarity measure, and

3. deriving the final list of point pairs consistent with an object model.

1.1 Selecting Distinct Points with an Interest Operator

In FBM instead of matching all pixels in an image, only selected points with certain features are to be matched. The selection principle should fulfill the following requirements:

- Distinctness: The points should be distinct, i.e. be different from neighbouring points. E. g. points on edges should not be selected if the epipolar geometry constraint is not used; also points in flat areas should not be selected. MORAVEC's and HANNAH's operators follow this aim: MORAVEC's operator (1977) searches for points with the largest minimum variance of gray level differences in 4 directions, while HANNAH's operator (1974) searches for points where the autocorrelation function of the gray level function is steep in all directions.
- Invariance: The selection as well as the selected position should be invariant with respect to the expected geometric and radiomatric distortions. This, besides the distinctness, probably is the most important requirement. The degree of invariance directly influences the precision and the reliability of the matching
- Stability: The selected points should be expected to appear in the other images. Thus the selection should be robust with respect to noise. In image sequence analysis the selected points should appear in long sequences of consecutive frames.
- Seldomness: Whereas distinctness guarantees local separability of points seldomness aims at global separability. This is essential in images with partially repetetive patterns. In order to avoid confusion elements of repetetive patterns should not be selected or at least should get a low weight. Thus the selection of seldom or interesting points leads to reliable results, explaining the notion "interst operator". A similar line of thought leads to the notion of salient features (cf. TURNEY et. al.).
- Interpretability: The selection principle should be interpretable in some sense, e. g. looking for edges, corners, blobs or other simple but labeled features. This requirement is not essential from an engineering point of view, but may be essential if the interest operator is used for image analysis.

The result of this first step are two lists with the n' and n" points selected in the two images I' and I", their pixel coordinates and their description, e. g. in the form of the local gray level function in the selected window. The advantage of the selection is obvious: it leads to a great information reduction, as we only have do deal with the two lists not with all pixels. It explains the requirements for the selection principle as the selected points reliably have to represent the total image content with respect to the matching problem.

Fig. 1 shows an artificial image pair. The black dots are the centres of the 7 by 7 windows selected by the new interest operator. The two lists of selected points with their weights are given in table 1. A closer look at fig. 1 reveils that the selected windows are not totally invariant as they appear at different places whithin the same corner. The reason for this seemingly deficiency and a remedy are discussed in section 4.

1.2 Preliminary Correspondence based on Similarity

From the n' x n" possible pairs of points only a few are pairs of corresponding points. In this step a preliminary list of candidate pairs is built, which is based on the similarity of the points. Points

are said to be similar if their description is similar. The similarity measure should fulfill the following requirements:

- Invariance: The similarity measure should be invariant with respect to the expected geometric and radiomatric distortions between the images. E. g. the correlation coefficient is invariant with respect to linear transformations of the gray values, but not with respect to geometric distortions.
  The problem with similarity measures is the form of the window which usually is chosen to be square or circular and which in general is not invariant with respect to scale differences or even shears. E.g. affine invariant moments (HU 1962) of the gray level function are invariant, only if the background is zero. Otherwise the noninvariance of the window form with respect to affine distortions, because of border effects, prevents the computed moments from being invariant (cf. GEISELMANN 1984). If at least scale differences between the images are to be expected the window size, possibly also its form, has to be adapted. The approach of BURNS et. al (1986) for extracting edges reflects this requirement as they first determine the edge region, i. e. the window, dependent on the local steepness of the edge, thus taking the - with respect to an ideal edge - local scale into account.
- Seldomness: The similarity measure should be able to include the seldomness of the individual points. Thus the degree of seldomness of both points in concern should also decide whether they remain in the preliminary list of the corresponding point pairs or at least should influence the weight of the correspondence.
- Heuristics: A priory knowledge may be incorporated in this step. E. g. the maximum parallax to be expected may be used to further reduce the number of candidate pairs. A special case would be the condition resulting from the known epipolar geometry reducing the search space by one dimension.
- Metric: For a thorough analysis it is convenient if the similarity measure has metric properties, i. e. besides being a distance measure it fulfills the triangle equation $d_{ij} \leq d_{ik} + d_{kj}$. This e. g. holds for the sum of squares of the gray level differences between the selected windows. A large distance d may correspond to a small similarity $s = 1/d$ or $s = 1-d$.

The preliminary list of candidate pairs, resulting from this step, is a further information reduction: Whereas in the previous step we still kept the full description of the individual points we now only need their position and the weight of the correspondence, unless it is needed for achieving consistency.

Table 2 shows the selected candidate pairs derived from table 1. The selection was based on the correlation coefficient of the gray level functions whithin the windows of the point pairs, which had to be > 0.5 and the maximum parallax, which was assumed to be 15 pixels in both directions.

1.3 Achieving Consistency

The local one-to-one comparison using the similarity measure and the heuristics in general is not able to yield a globally consistent matching result. Consistency here is understood as the fit of the data with respect to an object model or at least to a global model for the mapping function between the two images. In order to arrive at a final solution we therefore have to

1. provide a 3D-model of our object. The strength of the model directly influences the quality of the solution. The model may also be setup for the mapping function between the images, which - using the invers perspetive relations - can be then interpreted as a 3D-model. BARNARD and THOMPSON (1981) e. g. require the parallax

differences to be less or equal 1 pixel for points within a certain radius of a point in concern, say 15 pixels, also allowing exceptions. For the normal case of a stereo pair this is eqivalent to assuming the object surface to be piecewise horizontal or hardly sloped. Often the object model is not stated explicitely but is hidden in the algorithmic solution.

2. choose a consistency measure which is able to determine the closeness of fit of the data with the model. The choice of the target function is difficult in cases where different types of deviations between data and model have to be balanced. A classical problem is the proper relative weighting of the measuring errors, the smoothness of the surface and the frequency of discontinuities. A common theoretical framework, which e. g. allows maximum likelihood estimation, seems to be of great advantage for a thorough setup.
3. choose an algorithm to find a solution of optimal or at least satisfying consistency. There are various algorithms in use: In image sequence analysis nearest neighbourhood methods are very common (cf. KORIES 1986), they correspond to the minimal mapping approach proposed by ULLMAN (1979). Relaxation schemes as e. g. used by BARNARD and THOMPSON (1981) are very popular, as they may incorporate quite different types of consistency conditions. The clustering approach proposed by STOCKMAN et. al. (1982) shows intuitively that a global solution is aimed at.

Table 3 contains the final result of the new procedure. It is a robust estimation for the 6 parameters of an affine transformation between the two images, corresponding to a tilted plane as object model. All point pairs of the list of preliminary correspondencies together with their weights were introduced. The corresponding points are shown in fig. 2. The algorithm thus yields two results, which may be the basis for further analysis:

a. a list of pairs of points which are consistent with the global model and additional points in both images where point transfer promises to be accurate.
b. parameters of the mapping function, which allow a point transfer of other points, possibly not selected by the interest operator.

The next sections describe the three steps of the new procedure in detail.

2. Maximum Likelihood Estimation of the Mapping Function

The object model is setup in a parametric form to be able to estimate the parameters using maximum likelihood (ML) methods. This is no severe restriction as very general surfaces, specifically piecewise smooth surfaces can be represented in parametric form.

2.1 Object Model

For a first implementation of the algorithm a simple object model has been chosen. The surface of the object as far as it is shown in the images is assumed to be a tilted plane. This is a reasonable approximation if the images are not too large, say 40 x 40 to 120 x 120 pixels of size $(20\ \mu m)^2$. This object model is identical to a linear mapping function between the images. Thus in general we obtain the linear model for the parallaxes px = x" - x' and py = y" - y' of the corresponding points:

$$\begin{bmatrix} px_i + v_{px_i} \\ py_i + v_{py_i} \end{bmatrix} = \begin{bmatrix} \hat{a} & \hat{b} \\ \hat{d} & \hat{e} \end{bmatrix} \begin{bmatrix} x_i' \\ y_i' \end{bmatrix} + \begin{bmatrix} \hat{c} \\ \hat{f} \end{bmatrix}, \qquad D \begin{bmatrix} px_i \\ py_i \end{bmatrix} = \frac{1}{w_i} \begin{bmatrix} 1 & 0 \\ 0 & 1 \end{bmatrix} \qquad (2\text{-}1)$$

Solving for the 6 unknown parameters $\hat{a}$ to $\hat{f}$ yields the result of the 2D-matching result. In case the epipolar geometry is known we obtain d

= e = f = 0 if the parallaxes in the normal image are used. The parameter $\hat{a}$ measures the slope along the epipolar line, which is assumed to be roughly parallel to the x-axis, the parameter $\hat{b}$ measures the slope across the epipolar line, and $\hat{c}$ the parallax. If only points in one epipolar line are used for matching the parameter b has to be excluded, as it is not estimable. The 2D-matching in this case reduces to 1D-matching of a gray level line.

The model eq. (2-1) for the parallaxes is assumed to be valid for all corresponding points. The covariance, or dispersion matrix for the parallaxes depends on the type of the point, specifically its texture, and on the similarity between the left and the right image of the object point. Due to the selection principle of the interest operator for 2Dmatching the x- and y-parallaxes are assumed to be uncorrelated and of equal precision. Thus we have one weight for the parallaxes of each point pair.

The non corresponding point pairs can be treated as outliers with respect to the model. As we start from the list of preliminary correspondencies, not knowing the true ones, all parallaxes may be assumed to belong to a long tailed distribution. The most reasonable assumption for this distribution would be the outlier model $F = \alpha N + (1 - \alpha) H$ being a mixture of a normal distribution N and a very broard arbitrary distribution H. More simple approximations to F are the Laplace-Distribution $f(x) = c \exp(-|x|)$ or the Cauchy-Distribution $f = c / (1 + x^2)$.

2.2 ML-Estimation

In order to eliminate the effect of outliers onto the result one now can use ML or ML-type estimators. Then, instead of the (weighted) sum of the squares of the residuals v_i the sum of a less increasing function $\tau(v_i)$ is minimized (HUBER 1981):

$$\Sigma \tau(v_i) \Rightarrow \min \qquad (2\text{-}2)$$

which reduces to ML estimation if $\tau(x)$ is proportional to the negative logarithm of the density function.

Discussion:

1. Chossing $\tau(v) = v^2/2$ gives the least squares estimator, neglecting the weights for the moment.
2. Chosing $\tau(v) = |v|^p/p$ yields the estimator minimizing the L_p-norm. A special case is obtained for p = 1: Minimizing $\Sigma\tau(v) = \Sigma|v|$ is the well known least sum method being the ML-estimate for the Laplace-Distribution. It is the multiparameter version of the median.
3. The choice of τ can be guided by the socalled "Influence Curve" (IC) (HAMPEL 1973) being proportional to the derivative $\theta(v) = d\tau/dv$ of the minimum function. IC(v) or $\theta(v)$ give an indication how strong the influence of an outlier is onto the estimates in dependency of the size of the outlier.
4. The solution of eq. (2-2) can use existing programs for least squares solutions by either modifying the residuals or by modifying the weights, as

$$\Sigma\tau(v_i) = \Sigma \frac{\tau(v_i)}{v_i^2/2} \frac{v_i^2}{2} = \Sigma\, w(v_i) \frac{v_i^2}{2} \Rightarrow \min \qquad (2\text{-}3)$$

using the weight function

$$w(v_i) = \frac{\tau(v_i)}{v_i^2/2 + c} \quad (c \ll v_i^2/2) \qquad (2\text{-}4)$$

In an iterative solution the weights of all observations are updated depending on their residuals from the previous iteration.

5. If the function $\tau(v)$ is convex, thus $\theta(v)$ is non-decreasing, and

the model is linear then convergence is guaranteed under broard conditions (cf. HUBER, 1981, sect. 7.8).

Thus minimizing the L_1-norm seems to be optimal, as it is robust, and convergence is guaranteed. This method has, however, two disadvantages: 1.) $\tau(v)$ has no derivative at 0, thus, IC(v) is not continuous, which does not guarantee a unique solution and 2.) IC(v) = sign(v) is not zero for large values. Thus even large outliers have still an influence onto the result, which is not desirable. We therefor propose to use the following weight functions:

1. In order to ascertain convergence and a unique solution we slightly modify the minimum function of the L_1-norm (cf. fig. 3)

$$\tau_1(v) = 2\,(\sqrt{1 + v^2/2} - 1)$$
$$w_1(v) = 4\,(\sqrt{1 + v^2/2} - 1) \,/\, v^2 \qquad (2\text{-}5)$$
$$\theta_1(v) = v \,/\, \sqrt{1 + v^2/2}$$

   $\tau_1(v)$ is strictly convex with decreasing curvature for large v.

2. After having reached convergence, one can assume to have good approximate values for the parameters. In order to eliminate the influence of large outliers one could take one of the following minimum functions:

   Starting from a Cauchy-Distribution on obtains:

$$\tau_{2a}(v) = \ln(1 + v^2/2)$$
$$w_{2a}(v) = 2\ln(1 + v^2/2) \,/\, v^2 \qquad (2\text{-}6)$$
$$\theta_{2a}(v) = v \,/\, (1 + v^2/2)$$

   No convergence is guaranteed in the general case. Also as $\theta(v)$ is descending for large v, no unique solution is guaranteed if arbitrary approximate values are allowed. This is meaningful as the Cauchy-Distribution has neither mean nor variance.

   The following minimum function is proposed by KRARUP et. al. (1980) which considerably reduces the weights of false observations due to its exponential form:

$$\tau_{2b}(v) = v^2/2\,\exp(-v^2/2)$$
$$w_{2b}(v) = \exp(-v^2/2) \qquad (2\text{-}7)$$
$$\theta_{2b}(v) = v\,(1 - v^2/2)\,\exp(-v^2/2)$$

   This weight function fulfills practically all requirements for a well behaved weight function (HAMPEL 1973, WERNER 1984). It, however, cannot be derived from a density function, thus does not lead to a ML-estimate.

The functions are shown in fig. 3 together with the minimum-, weight- and influence-function of the least squares $\tau_0(v) = v^2/2$.

2.3 Algorithmic Solution

In each iteration of this robust estimation, the parameters, the residuals, the precision of the estimates and the average weight are determined, and the weights are adapted for the next iteration. If a weight is smaller than a certain percentage (say, 10 %) of the average weight, it is set to zero, eliminating this point. The first few (3 or 4) iterations are performed with the weight function w_1, after which the redescending function w_{2b} is applied. The algorithms stops if either the reqired precision of the parameters is reached, not enough corresponding points are left, or a preset number of iterations is reached. The residuals of the last iteration are then tested and with all points passing this test one additional iteration with equal

weights is performed to obtain the final parameters.

The obtained list of corresponding points may then still be ambiguous, as the same point in one image might correspond to several points of a cluster in the other image. The list of pairs of points is then cleaned keeping those correspondencies which have the smaller residuals (cf. table 3).

The result obtained this way has to be checked independently in order to be able to guarantee for its correctness. For this purpose a global correlation coefficient is calculated from the gray levels of a regular grid, taking the estimated mapping into account. If this correlation coefficient is below 0.5 the result is rejected, which may be caused e. g. by non-sufficient approximate values. We made the experiance that this indicator is very reliable: it never suggested a false solution to be correct.

3. Similarity Measure

The estimation procedure requires initial weights for the observations which in our case are the parallaxes of the point pairs in the list of preliminary correspondencies. Hence the majority of the observations are outliers and assuming equal weight would prevent the solution from getting started.

Now the weights can be obtained from the covariance matrix of the estimated shifts if we would apply LSM to all point pairs. It is given by (cf. FÖRSTNER 1986):

$$C = D\begin{bmatrix} px \\ py \end{bmatrix} = \hat{\sigma}^2_{\Delta g} \begin{bmatrix} \Sigma\, g_x^2 & \Sigma\, g_x \cdot g_y \\ \Sigma\, g_y \cdot g_x & \Sigma\, g_y^2 \end{bmatrix}^{-1} = \hat{\sigma}^2_{\Delta g}\, Q \qquad (3\text{-}1)$$

where g is the gray level function of the object, restored from g' and g'', $\hat{\sigma}_{\Delta g}^2$ is the estimated variance of the gray level differences thus the noise, and g_x and g_y are the derivatives in x- and y-direction resp.. The sums are to be taken over all pixels of the window around the points in concern.

The covariance matrix fully describes the precision of the match between the gray level functions g' and g'' and can be visualized by an error ellipse. A good match therefore must fulfill the following two reqirements:

C1: the error ellipse should be close to a circle, otherwise the match is not well dfined in one direction, e. g. at an edge.
C2: The error ellipse should be small.

The interest operator is based on these two criteria. As the covariance matrix directly measures the curvature of the 2D-autocovariance function within the window, the interest operator, except for the normalization, is essentially identical with HANNAH's operator. It is however, much more simple to be calculated.

We now can assume the error ellipses of all selected points to be close to a circle. Then the weight can be directly derived from the trace of the covariance matrix:

$$w = 1 \,/\, \mathrm{tr}\,(C) = 1 \,/\, (\hat{\sigma}^2_{\Delta g}\ \mathrm{tr}\,(Q)\,) \qquad (3\text{-}2)$$

Observe, that the trace is invariant to rotations. Taking the gray level differences directly to estimate $\hat{\sigma}_{\Delta g}^2$ has the disadvantage of being biased if the two images have different brightness or contrast. The correlation coefficient is known to be a better measure. Now, if one, for simplicitity, assumes the images g' and g'' to be related to

the true image g by $g' = a' (g + n') + b'$ and $g'' = a'' (g + n'') + b''$ with $\sigma^2_{n'} = \sigma^2_{n''} = \sigma^2_n$ where a and b represent contrast and brightness, the signal to noise ratio $SNR^2 = \sigma_g^2/\sigma_n^2$ is functionally related to the correlation coefficient r by:

$$r = \frac{\sigma_{g',g''}}{\sigma_{g'}\sigma_{g''}} = \frac{\sigma_g^2}{\sigma_g^2 + \sigma_n^2} = \frac{SNR^2}{SNR^2 + 1} \quad \text{or} \quad SNR^2 = \frac{r}{1 - r} \qquad (3\text{-}3)$$

By using the approximations $\Sigma n_i^2 \approx N \sigma_n^2$ (N being the number of pixels in the window), $\sigma_g^2 \approx \sigma_{g'} \sigma_{g''}$, $tr\, Q \approx \sqrt{tr\, Q'\ tr\, Q''}$ and $\sigma_{\Delta g}^2 \approx 2 \sigma_n^2$ we obtain the following relation for the weight of the parallaxes:

$$w \approx \frac{N}{2}\ \frac{r}{1 - r}\ \frac{1}{\sigma_{g'}\ \sigma_{g''}}\ \frac{1}{\sqrt{tr\, Q'\ tr\, Q''}} \qquad (3\text{-}4)$$

Discussion:

1. The weight depends on four terms. The number N of pixels in the windows is equal for all points, thus can be neglected. The second one reflects the similarity between the two points in concern and needs to be calculated for all pairs of points. Actually only those correlation coefficients are calculated where the parallaxes are less than a prespecified task dependent threshold. The other terms depend on values obtainable separately from both images and are provided from the interest operator.
2. The traces tr Q' and tr Q'' measure the distinctness or the locatability of the points and are critical for the selection of appropriate points. The reason is, that the noise level can reasonably be assumed to be constant in both images (cf. eq. 3-2).
3. The weight is a generalization of the one used by BARNARD and THOMPSON (1981). It is independent of brightness and contrast and takes the texture of the points into account.
4. A simple and reasonable criterion to reject pairs of points based on the correlation coefficient is $r < 0.5$. This is equivalent to requiring SNR to be larger than 1.
5. As the correlation coefficient, thus the similarity measure is not invariant with respect to scale, rotation and shear, the approximate values for these unknown parameters still have to be better than 30 %.
6. However, the separation of the different terms in eq. (3-4) has the advantage in its ability to include other measures of similarity. The correlation coefficient needs not be derived from gray levels but may use other features of the points, e. g. one could use a small set of features just to decrease the computing time, e. g. the low frequency terms of a cosine transformations or one could use structural information, the result of a classification or a linguistic description in combination with statistical measures, in order to obtain invariance with respect to the expected geometric distortions. The only requirement for the measure is to have the properties of a correlation coefficient, or r/(1-r) to be a metric distance measure.

4. The Interest Operator

The interest operator has to find points with the two req rements for the error ellipse which one would obtain from point transfer: C1: it should be close to a circle and C2: it should be small. Now, the error ellipse can only be calculated using a the gray levels within a certain window, which usually is chosen 5 x 5 or 7 x 7 pixels. The centre of the window in general is not the best point for matching, as the transformation of this point is not invariant to geometric distortions (cf. fig. 4a). An optimal point within the window is the weighted centre of gravity, which proves to have attractive features.

4.1 Selecting an Optimal Window

We have required that the error ellipse representing the covariance matrix of the parallaxes is close to a circle. Moreover, we require that the point can well be located. Measures of both requirements (C1 and C2), should, in a simple way, be derivable from the gray level function of the image patch, as they are to be determined for all pixels, i. e. all possible positions of a small window within the images.

Now the eigenvalues of the covariance matrix are invariant to rotations. We will use them to determine the closeness of the error ellipse to a circle. Moreover, the eigenvalues of the coefficient matrix, say Q', and those of the inverse N' = (Q')$^{-1}$ are related by $\mu_i(Q') = 1/\mu_i(N')$. Thus, let μ_1 and μ_2 be the eigenvalues of N', then the ratio

$$q = \frac{4 \det N'}{(\mathrm{tr}\, N')^2} = \frac{4\,\mu_1\,\mu_2}{(\mu_1 + \mu_2)^2} = 1 - \left(\frac{\mu_1 - \mu_2}{\mu_1 + \mu_2}\right)^2 \qquad (4\text{-}1)$$

is an adequate measure for the roundness of the error ellipse. If q = 0 (and not both μ_1 and μ_2 are zero) then det N' is zero and the matrix is singular. This means that g_x and g_y are linearliy dependent thus the point may ly on an edge (cf. NAGEL/ENKELMANN 1986). The case q = 1 is reached only if the eigenvalues are equal thus representing an error circle. The calculation of q needs not use the eigenvalues, but rather the determinant and the trace of N' which can be derived from the sums Σg_x^2, Σg_y^2 and $\Sigma g_x g_y$. We also do not need to invert N'.

Similarily we can derive an expression for tr Q':

$$\mathrm{tr}\, Q' = \mathrm{tr}\, N' \,/\, \det N' \qquad (4\text{-}2)$$

Thus the selection of the optimal windows can be accomplished for both images separately in the following steps:

1. Determination of the elements of N, which essentially are three convolutions, namely of the three derived images $g_x^2(i,j)$, $g_y^2(i,j)$ and $g_x(i,j) \cdot g_y(i,j)$, with a separable kernel containing only 1's, which needs just 4 additions per pixel if calculated recursively.
2. Determination of tr Q and of q using eq. (4-1) and (4-2).
3. Determination of the interest value, being a preliminary weight for each pixel:
$$\bar{w} = \begin{cases} 1 \,/\, \mathrm{tr}\, Q \text{ if } q > q_{min} \text{ (e. g. 0.5)} \\ 0 \text{ else} \end{cases} \qquad (4\text{-}3)$$
4. Suppression of all local non-maxima by setting the function $\bar{w}(i,j)$ to 0 at local non-maxima.
5. Extraction of all windows for which $\bar{w}(i,j)$ is not 0.

Until recently we treated the centres of the windows as selected points. The example given in section 1 is based on this selection principle. For images with sharp edges this selection principle reveals severe deficiencies increasing with larger window sizes, which has also been discussed by DRESCHLER (1981). There a specialized interest operator for finding corners has been developped. This seems to be too restrictive for general imagery. We therefore follow a different approach.

4.2 Selecting Optimal Points

The selection of optimal windows was based on the expected precision of LSM. By taking the relative maxima of w, the expected precision using the small window is better than the precision obtainable with all neighbouring windows. Now it can be shown that this selection principle also yields optimal precision for three other tasks, which lead to a normal equation matrix N with the same eigenvalues:

1. The determination of the weighted centre of gravity $z = (x, y)^t$ of the window leads to the following model:

$$\begin{aligned} x_i + v_i &= \hat{x} \\ y_i + v_i &= \hat{y} \end{aligned} \qquad W_i = \begin{bmatrix} g_{xi}^2 & g_{xi} \cdot g_{yi} \\ g_{xi} \cdot g_{yi} & g_{yi}^2 \end{bmatrix} \qquad (4\text{-}4)$$

Thus each pixel contributes to the weighted centre of gravity according to the size and direction of the local gradient.

The same equation system would be obtained for LSM if x_i and y_i would mean local, i. e. pixelwise estimates for the shifts x and y from $x_i = (g_i'' - g_i') / g_{xi}$ and $y_i = (g_i'' - g_i') / g_{yi}$. Because derived from the same gray level difference they are 100 % correlated with the weight matrix in eq. (4-4).

2. The determination of the intersection of all gray level edges in the window leads to the following model:

$$d_i + v_i = \cos \alpha_i \; \hat{x} + \sin \alpha_i \; \hat{y} \qquad D(d_i) = g_i'^2 \qquad (4\text{-}5)$$

with $\tan \alpha_i = g_{yi}/g_{xi}$, $d_i = x_i \cos \alpha_i + y_i \sin \alpha_i$, and $g_i'^2 = g_{xi}^2 + g_{yi}^2$. Thus each individual edge-element contributes to the intersection point according to the square of the magnitude of the gradient.

3. The determination of the intersection of all local lines of steepest descent, thus of slope-elements, within the window leads to the following model:

$$d_i + v_i = -\sin \alpha_i \; \hat{x} + \cos \alpha_i \; \hat{y} \qquad D(d_i) = g_i'^2 \qquad (4\text{-}6)$$

with the same abbreviations as before. Thus each individual slope-element, which is perpendicular to the local edge-element, contributes to the intersection point according to the square of the magnitude of the gradient. If the gray level function is consisting of one or several circularily formed edges the intersection of the slope-elements is the centre of these circles.

Discussion:

1. The selection of windows, which are optimal for matching are also optimal for determining the weighted centre of gravity, the intersection point or the centre of a circle or a set of rings.
2. The numerical solutions of problem 1. and 2. coincide, i. e. the weighted centre of gravity is identical to the intersection of all edges in the window. This can be seen by setting up the normal equations. The solution is $\hat{z} = (\Sigma W_i)^{-1} \Sigma(W_i z_i)$, with $z_i = (x_i, y_i)^t$.
3. The estimation of the images of corner points of polyhedra is invariant to rotations in space, if based of the model eq. (4-5). This is probably the most far reaching consequence of this derivation.
4. The number of edges within a window needs not to be known in advance in order to be able to estimate the intersection point (cf. fig. 5: 1-6,13-15)
5. Similarily the number of edge-rings within a window needs not to be known in advance (cf. fig. 5: 10-12)
6. Also mixtures of intersecting edges and lines can be determined. Moreover, the end point of a line can be estimated due to the existence of an edge-element at the end of the line (cf. fig. 5: 7-9, 16-18).
7. The ML-estimate provides the precision of the estimated point. The standard deviations of the estimated coordinates usually are below 1/4 of a pixel.
8. The classification of the point can be based on the closeness of fit with respect to the 3 models (general point, intersection point, centre of rings), which has not performed in the examples in fig. 5.

Fig. 4 shows the centre of the selected windows (4.a) and the selected points (4.b) for a checker bord in two orientations. Nearest neighbourhood resampling was used for the rotated one. In fig. 5 several image patches are shown together with the edge- or slope-elements, the estimated point and the confidence ellipse derived from the fit of the gray levels with respect to the model. The true point with a probability of 99 % lies within the confidence ellipse, provided the model holds. The edge- and slope elements are positioned between the pixels as Roberts gradient has been used. The examples clearly demonstrate the capabilities of the point selector.

4.3 A Measure for Seldomness

The preliminary weight $\bar{w} = 1 / \mathrm{tr}\, Q$ (eq. 4-3) for the points selected this way only takes the local gray level function into account, thus is independent on the other selected points. In images with repetetive patterns one, however, should give those points a higher weight whose features are seldom, in order to increase the reliability of the initial estimate.

The problem of finding seldom, thus specific structures for matching is a very general one. There are basicly two solutions:

a. The supervised selection of features uses the information of correct matches of a representative sample. Thus those features are selected, which in a training phase gave best results. The approach by KAK et. al. (1986) follows this line.
b. The unsupervised selection of features is based only on the mutual similarity of the points or objects in concern, specifically how dissimilarity can be expexted to influence the matching result. The approach by TURNEY et. al. (1985) follows this line.

For supervised selection the representativity of the training sample is crucial, whereas for unsupervised selection the underlying mathematical model for matching is decisive. We are only interested in a relative weighting of the points and , because of the inherent limitations of training procedures, do not want to rely on a - possibly large - set of correct matches. We therefore propose the following simple method for measuring the seldomness of the selected points, which can be derived after the selection from the set of points in each of the images alone.

Seldom points have features which are different or dissimilar from those of all other points. As we used the correlation coefficient for measuring the similarity of points in different images we now also use the correlation coefficient for measuring the similarity (or dissimilarity) between points within one image. Let $R = (r_{ij})$ be the correlation matrix of all selected points within one image, derived from the gray levels within the window around the points. Then the seldomness S_i of point i, similarily to eq. (3-3) for SNR, can be obtained from:

$$S_i = (1 - r_i) / r_i \quad \text{for } r_i > 0,\ S_i = \infty \text{ else} \qquad (4\text{-}6)$$

where r_i is a correlation coefficient measuring the similarity of point i with all other points. There are at least two choices at hand for deriving such a summarizing value:

$$1. \quad r_i = \max_{j \neq i} (r_{ij}) \qquad (4\text{-}7.1)$$

$$2. \quad r_i'^2 = 1 - [(R^{-1})_{ii}]^{-1} = r_i^t R^{-1} r_i \qquad (4\text{-}7.2)$$

The first choice r_i just measures the maximum similarity of i with all other points j. The second choice r_i' is the socalled total correlation, which for instance is proposed by JACOBSEN (1982) for evalua-

ting the mutual dependency of additional parameters for selfcalibration. It needs the diagonal elements of the inverse of the correlation matrix. In eq. (4-7.2) r_i is the i-th column of R without the diagonal element $R_{ii} = 1$, and R_i is the correlation matrix without row and column i. Obviously r_i' is the weighted average of all correlations of point i with the other points. r_i' is theoretically more attractive than r_i, as it measures the separability of point i and the other points (cf. FÖRSTNER 1983). It can be algebraicly related to the information theoretic notion of seldomness in the sense of low probability. This is, because for small r_i', thus for a point well separable from the others, the information, measured in bits, necessary to describe this point, given the others, is large, indicating the point to be a seldom one. This forms a link to the supervised selection principle for structural features proposed by KAK et. al. (1986).

But, as can seen from 2 x 2 matrices, for which $r_1' = r_2' = |R_{12}|$ holds, r_i' cannot discern positive and negative correlations. We therefore propose to use the, also more simple measure r_i for deriving the seldomness.

In both cases large correlations between the points, thus large off-diagonal elements in R lead to large summarizing correlation coefficients r_i, thus to small seldomness measures, as should be expected.

Example: The correlations of the 3 first windows of fig. 5 are $r_{12} = 0.92$, $r_{13} = 0.29$ and $r_{23} = 0.39$. We obtain:

1: S1 = 0.09, S2 = 0.09, S3 = 1.56
2: S1' = 0.43, S2' = 0.40, S3' = 2.29

both choices indicating the third window to have the most seldom characteristics from these three windows, which corresponds to intuition. The total correlations are $r_1'^2 = 0.85$, $r_2'^2 = 0.86$ and $r_3'^2 = 0.16$. ■

The preliminary weight $\bar{w}_i$ from eq. (4-3) of each point can now be corrected for seldomness by multiplying it with S_i. Altogether the weight of a preliminary correspondence between point i in image I' and j in image I" with eq. (3-4) now can then be written as:

$$w_{ij} \approx \frac{N}{2} \frac{r_{ij}}{1 - r_{ij}} \frac{1}{\sigma_{g_i'} \cdot \sigma_{g_i''}} \sqrt{\bar{w}_i \cdot \bar{w}_j} \cdot \sqrt{S_i \cdot S_j} \qquad (4\text{-}8)$$

The main effort for deriving these weights is the calculation of the correlation coefficients of the points within and between the images.

5. Conclusions

The feature based matching algorithm described above has been implemented on a photogrammetric measuring device, a Zeiss Planicomp C100, within the program PALM (SCHEWE/FÖRSTNER 1986) for automatic line and surface measurments developped for the mensuration of car body surfaces. The algorithm supports the least squares matching algorithm by providing reliable and accurate approximate values if necessary. The precision of this FBM procedure has been shown to be appr. 1/3 of a pixel in case the centre of the selected windows are used as feature points and the images show enough texture. The time for matching two images of 120 x 120 pixels is about 2 seconds on a VAX 11/780. On an HP1000 A900 computer the time for two images of 40 x 40 pixels is appr. 8 seconds. The accuracy can be expected to be significantly better if the weighted centres of the windows according to sect. 4.2 are used as feature points, then yielding accuracies which may be sufficient for robot control or inspection tasks. The concept is able to include a similarity measure, being invariant to the expected geometric distortions without changing the interest operator and to

extend the object model to much more general surfaces. The ability of the interest operator to find and accurately locate corners with arbitrary number and orientation of edges or lines need further investigation, specifically for supporting image analysis.

References:

BARNARD S. T., THOMPSON W. B. (1981): Disparity Analysis of Images, IEEE, Vol. PAMI -2, 1981, pp. 333-340

BURNS J. B., HANSON A. R., RISEMAN E. M. (1986): Extracting Straight Lines, IEEE, Vol. PAMI-8, No. 4, 1986, pp. 425-455

DRESCHLER L. (1981): Ermittlung markanter Punkte auf den Bildern bewegter Objekte und Berechnung einer 3D-Beschreibung auf dieser Grundlage, Diss. Fachber. Informatik, Univ. Hamburg, 1981

FÖRSTNER W. (1983): Reliability and Discernability of Extended Gauss-Markov Models, Deutsche Geod. Komm., A 98, München 1983

FÖRSTNER W., PERTL A. (1986): Photogrammetric Standard Methods and Digital Image Matching Techniques for High Precision Surface Measurements, Pattern Recognition in Practice II, North Holland, 1986

FÖRSTNER W. (1986): Digital Image Matching Techniques for Standard Photogrammetric Applications, ASP-ASCM Convention, Washington D. C., 1986

GEISELMANN Ch. (1984): Untersuchungen zur Berücksichtigung von affinen Verzerrungenbei der Oberflächenzuordnung mit Invarianten, Diplomarbeit am Inst. f. Photogr., Stuttgart, 1984

HAMPEL F. R. (1973): Robust Estimation, A Condensed Partial Survey. Zur Wahrscheinlichkeitstheorie 1973

HANNAH M. J. (1974): Computer Matching of Areas in Stero Images, PH. D. Thesis, Memo AIM 219, Stanford University, Stanford/CA

HU M. K. (1962): Visual Pattern Recognition by Moment Invariants, IRE Trans. Info. Theory, Vol. IT-8, pp. 179-187

HUBER P. J. (1981): Robust Statistics, New York 1981

JACOBSEN K. (1982): Selection of Additional Parameters by Program, Int. Arch. f. Phot., Vol.24-III, Helsinki 1982, pp.266-275

KAK A. C., BOYER K. C., CHEN C. H., SAFRANEK R. J., YANG H. S. (1986): A Knowledge-based Robotic Assembly Cell, IEEE Expert, pp. 63-83

KORIES R. R. (1986): Bildzuordnungsverfahren für die Auswertung von Bildfolgen, Schriftenr. d. Inst. f. Photogrammetrie, Heft 11, Stuttgart 1986

MORAVEC H. P. (1977): Towards Automatic Visual Obstacle Avoidance, IJCAI-77, p 584

NAGEL H.-H., ENKELMANN W. (1986): An Investigation of Smoothness Constraints for the Estimation of Displacements vector Fields from Image Sequences, IEEE, Vol. PAMI-8, No. 5, pp. 565-593

PADERES F. C., MIKHAIL E. M., FÖRSTNER W. (1984): Rectification of Single and Multiple Frames of Satellite Scanner Imagery using Points and Edges as Control, NASA Sympos. on Mathematical Pattern Recognition and Image Analysis, June 1984, Houston

SCHEWE H., FÖRSTNER W. (1986): The Program PALM for Automatic Line and Surface Measurement Using Image Matching Techniques, Int. Arch. of Photogr., Vol. 26-III, Rovaniemi 1986, pp. 608-622

STOCKMAN G. C., KOPSTEIN S., BENETT (1982): Matching Images to Models for registration and Object Location via Clustering, IEEE, Vol. PAMI-4, No. 3, 1982, pp. 229-241

TURNEY J. L., MUGDGE T. N., VOLZ R. A. (1985): Recognizing Partially Occluded Parts, IEEE Vol. PAMI-7, No. 4, July 1985, pp. 410-421

ULLMAN S. (1979): The Interpretation of Visual Motion, The MIT Press, Cambridge, 1979

WERNER H. (1984): Automatic Gross Error Detection by Robust Estimators, Int. Arch. of Photogr. and Remote Sensing, Vol. 25-III, Rio de Janeiro, 1984

Acknowledgements: This research has been partly supported by NASA Contract No. 9-16664 through Subcontract No. L200074 with Texas A&M Research Foundation and by the Deutsche Forschungsgemeinschaft. I want to thank Prof. E. M. Mikhail for his valuable support and for the opportunity to work at his institute at Purdue University.

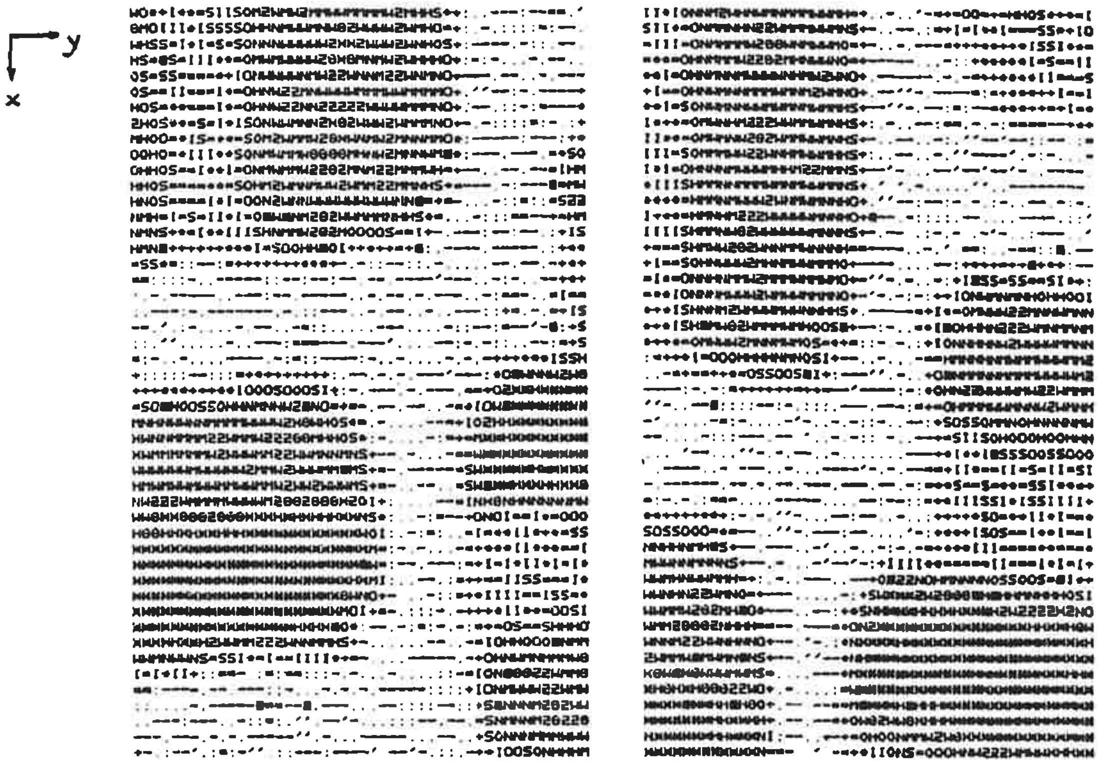

Figure 1 Artificial Image Pair With Selected Points (black pixels)

NOTE: Window size of interest operators: 7

Window size for non-maximum suppression: 3

Left Image

i	x	y	$\bar{w}$	q
1	4	4	387	91
2	10	34	410	49
3	12	49	907	67
4	13	31	364	43
5	14	13	410	67
6	14	17	450	39
7	16	4	714	88
8	16	21	483	39
9	16	31	345	34
10	21	45	961	62
11	24	41	964	40
12	26	4	316	37
13	26	19	622	64
14	26	46	963	31
15	30	23	448	33
16	31	38	1871	94
17	34	29	1518	88
18	40	22	867	30
19	41	45	311	88
20	43	40	640	78
21	45	14	384	38
22	43	19	327	37
23	48	39	686	78

Right Image

i	x	y	$\bar{w}$	q
1	14	28	311	36
2	16	45	308	49
3	17	42	288	39
4	18	36	688	71
5	21	7	586	78
6	21	22	469	63
7	21	33	423	63
8	24	18	443	61
9	24	23	708	59
10	26	6	280	48
11	29	38	323	88
12	33	8	718	74
13	37	37	1374	63
14	37	43	368	46
15	38	36	308	38
16	38	38	340	34
17	39	11	314	37
18	42	4	389	86
19	42	11	376	48
20	43	4	301	81
21	44	3	379	77
22	46	10	446	39
23	48	24	1682	88
24	48	29	344	43

Table 1 List of Selected Points

NOTE: x,y coordinates

$\bar{w}$ interest value

q measure for isotropy of error ellipse (in percent)

	i	j	w	$\bar{w}_i$	$\bar{w}_j$	rho
1	2	01	4.737	410.	311.	0.813910
2	2	06	18.307	410.	469.	0.734148
3	3	07	6.047	907.	423.	0.743084
4	3	09	9.129	907.	708.	0.769720
5	4	06	3.383	364.	469.	0.733839
6	4	08	8.666	364.	443.	0.872919
7	5	05	27.938	410.	586.	0.932111
8	5	10	2.082	410.	280.	0.372882
9	6	05	16.436	450.	586.	0.883114
10	6	08	2.738	450.	443.	0.632202
11	7	08	16.076	714.	443.	0.893975
12	8	08	11.647	483.	448.	0.899358
13	8	10	1.838	483.	280.	0.589371
14	9	06	4.533	345.	469.	0.777062
15	9	08	11.360	345.	443.	0.899266
16	9	11	2.187	345.	323.	0.599432
17	10	02	2.891	961.	300.	0.611310
18	10	03	2.454	961.	288.	0.611800
19	10	04	2.378	961.	688.	0.519324
20	10	07	2.692	961.	423.	0.362607
21	11	02	2.333	964.	300.	0 613341
22	11	03	8.660	964.	288.	0.874139
23	11	04	38.190	964.	688.	0.966364
24	11	07	2.328	964	423.	0.601318
25	11	13	133.224	964.	1374.	0.983662
26	11	14	3.310	964.	368.	0.681337
27	11	15	13.244	964.	308.	0.891736
28	11	16	7.161	964.	340.	0.812974
29	12	12	4.827	316.	718.	0.776938
30	13	12	22.732	622.	718.	0.919691
31	13	13	7.178	622.	1374	0.764347
32	13	17	1.891	622.	314.	0.579380
33	14	03	2.998	963.	288.	0.689992
34	14	04	11.141	963.	688.	0.843669
35	14	07	9.303	963.	423.	0.745871
36	14	09	2.978	963.	708.	0.537126
37	14	13	15.047	963.	1374.	0.861033
38	14	15	4.797	963.	308.	0.732863
39	14	16	3.142	963.	340.	0.638196
40	15	12	7.280	448.	718.	0.800946
41	15	15	2.030	448.	308.	0.584841
42	15	16	2.129	448.	340.	0.589807
43	15	17	12.494	448.	314.	0 908979
44	15	19	26.556	448.	376.	0.943766
45	15	22	11.948	448.	446.	0.874251
46	16	09	9.838	1871.	708.	0.746461
47	16	11	3.381	1871.	323	0 336839
48	16	23	129 159	1871.	1682.	0.970396
49	17	06	16.139	1518.	469.	0.879777
50	17	08	2.468	1518.	443.	0.333913
51	17	17	6.066	1518.	314.	0.764804
52	17	19	4.692	1518.	376.	0.683444
53	18	10	1.367	867.	280.	0.304329
54	18	24	5.183	867.	344.	0.779709
55	19	14	3.144	311.	368.	0.693980
56	19	15	7.749	311.	308.	0.843612
57	19	16	6.314	311.	340.	0.810626
58	20	13	3.123	640.	1374.	0 631036
59	23	23	29.446	686.	1682.	0.911693

Table 2 List of Selected Pairs

NOTE: ij point No. in left and right image (201 ≙ (2,1)), w initial weight, $\bar{w}$ preliminary weights, rho correlation coefficient.

$$\begin{pmatrix} 1.19529 & 0.10307 & ; & 3.58 \\ -0.08767 & 0.88201 & ; & -4.45 \end{pmatrix}$$

a)

i	left	right	xl	yl	xr	yr	dx	dy
1	2	6	10.000	34.000	21.000	22.000	-1.961	0.637
2	3	7	12.000	45.000	21.000	33.000	1.563	-0.840
3	3	9	12.000	45.000	24.000	33.000	-1.437	-0.840
4	4	8	13.000	31.000	24.000	18.000	-1.684	1.722
5	8	10	16.000	21.000	26.000	8.000	-1.129	2.633
6	9	8	16.000	31.000	24.000	18.000	1.902	1.453
7	11	13	24.000	41.000	37.000	27.000	-0.505	0.556
8	13	12	26.000	19.000	35.000	8.000	1.618	-0.027
9	14	13	26.000	40.000	37.000	27.000	1.782	-0.505
10	15	17	30.000	23.000	39.000	11.000	2.811	0.142
11	15	19	30.000	23.000	42.000	11.000	-0.189	0.142
12	15	22	30.000	23.000	45.000	10.000	-3.189	1.142
13	16	23	31.000	38.000	45.000	24.000	-0.448	0.282
14	5	5	14.000	15.000	21.000	7.000	0.862	-1.480
15	13	17	26.000	19.000	39.000	11.000	-2.382	-3.027
16	6	5	14.000	17.000	21.000	7.000	1.048	0.284
17	4	6	13.000	31.000	21.000	22.000	1.316	-2.278

clean list

b)

i	left	right	xl	yl	xr	yr	dx	dy
1	2	6	10.000	34.000	21.000	22.000	-1.961	0.637
2	3	9	12.000	45.000	24.000	33.000	-1.437	-0.840
3	8	10	16.000	21.000	26.000	8.000	-1.129	2.633
4	9	8	16.000	31.000	24.000	18.000	1.902	1.453
5	11	13	24.000	41.000	37.000	27.000	-0.505	0.556
6	13	12	26.000	19.000	35.000	8.000	1.618	-0.027
7	15	19	30.000	23.000	42.000	11.000	-0.189	0.142
8	16	23	31.000	38.000	45.000	24.000	-0.448	0.282
9	4	5	14.000	17.000	21.000	7.000	1.048	0.284

Table 3 Result of Robust Affine Transformation

a) uncleaned list, containing ambiguities
b) cleaned list, final result
(cf. Figure 2)

NOTE: 6 iterations

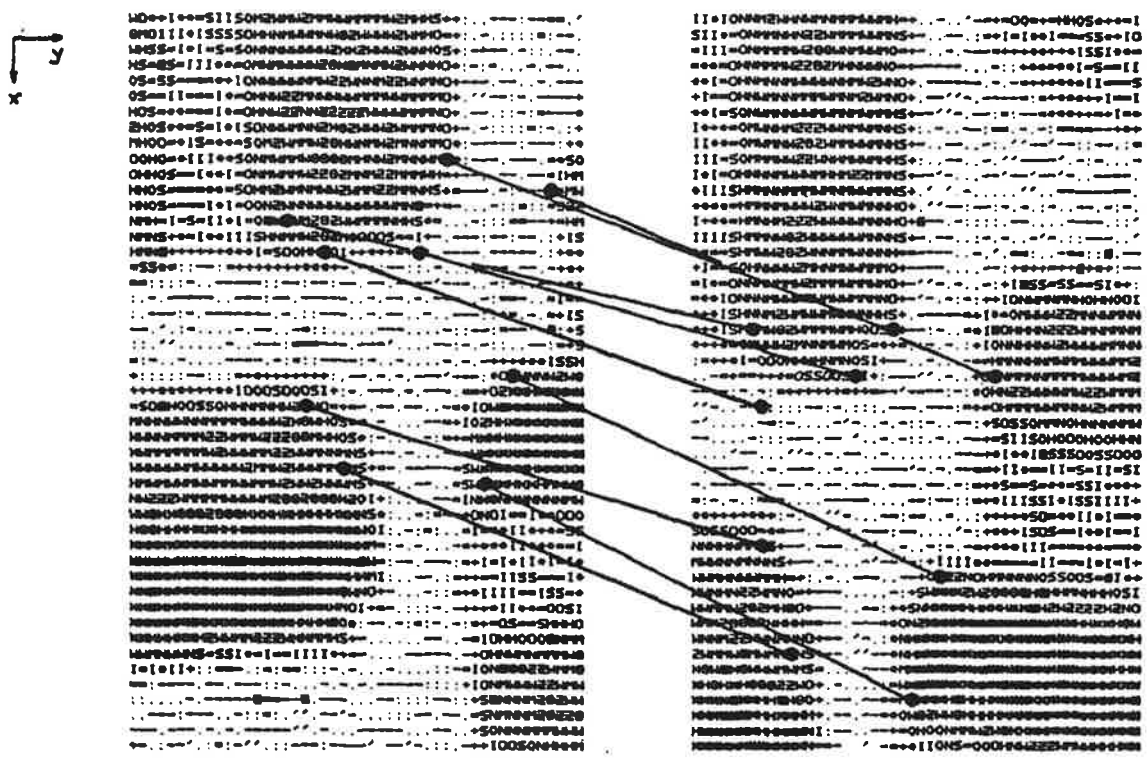

Figure 2 Result of Correspondence Algorithm.

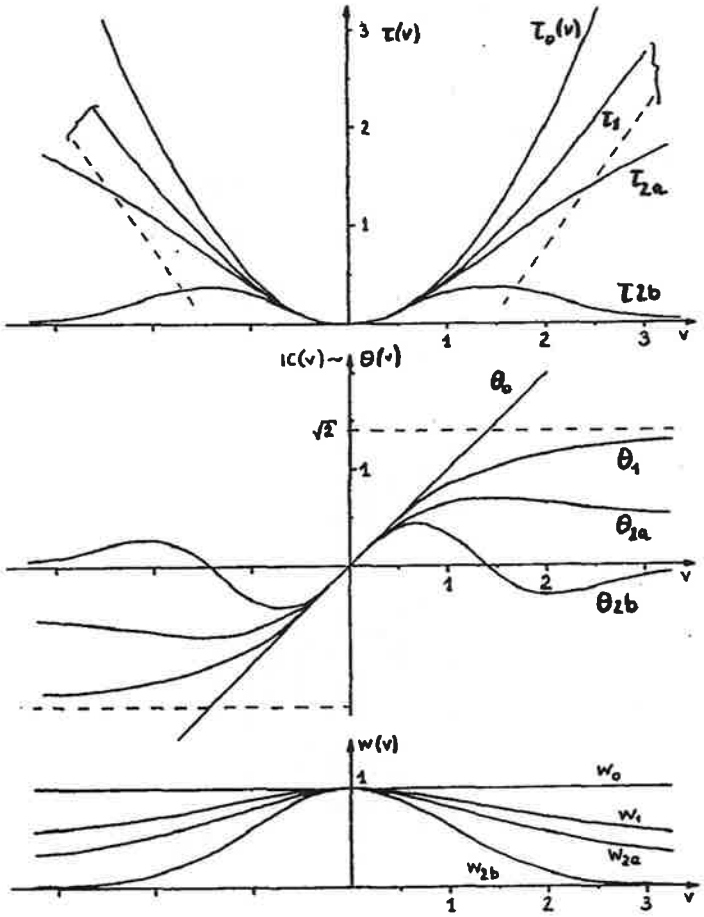

Figure 3 Minimum, Influence, and Weight Functions $\tau(v)$, $IC(v)\sim\vartheta(v)$, and $w(v)$.

NOTE: 0: least squares, non robust ($\vartheta(v)$ not bounded)

1: L_1-Norm, robust, convergence guaranteed

2: redescending IC,
- a: ML-estimator for Cauchy-Distribution
- b: exponential weight-function

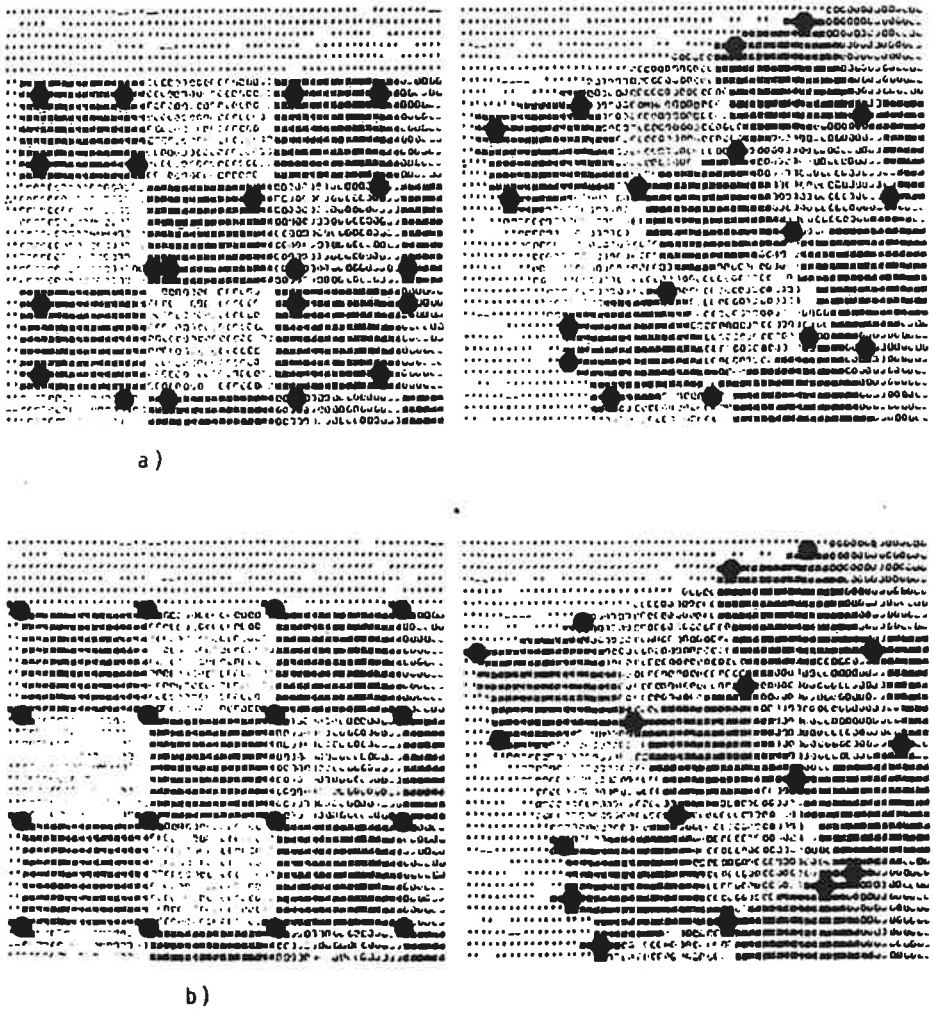

Fig. 4 Result of interest operator on checker board
Nearest neighbourhood resampling for rotated board
a) center of selected windows
b) estimated corners = weighted center within selected windows
NOTE: Several windows contain the same corner

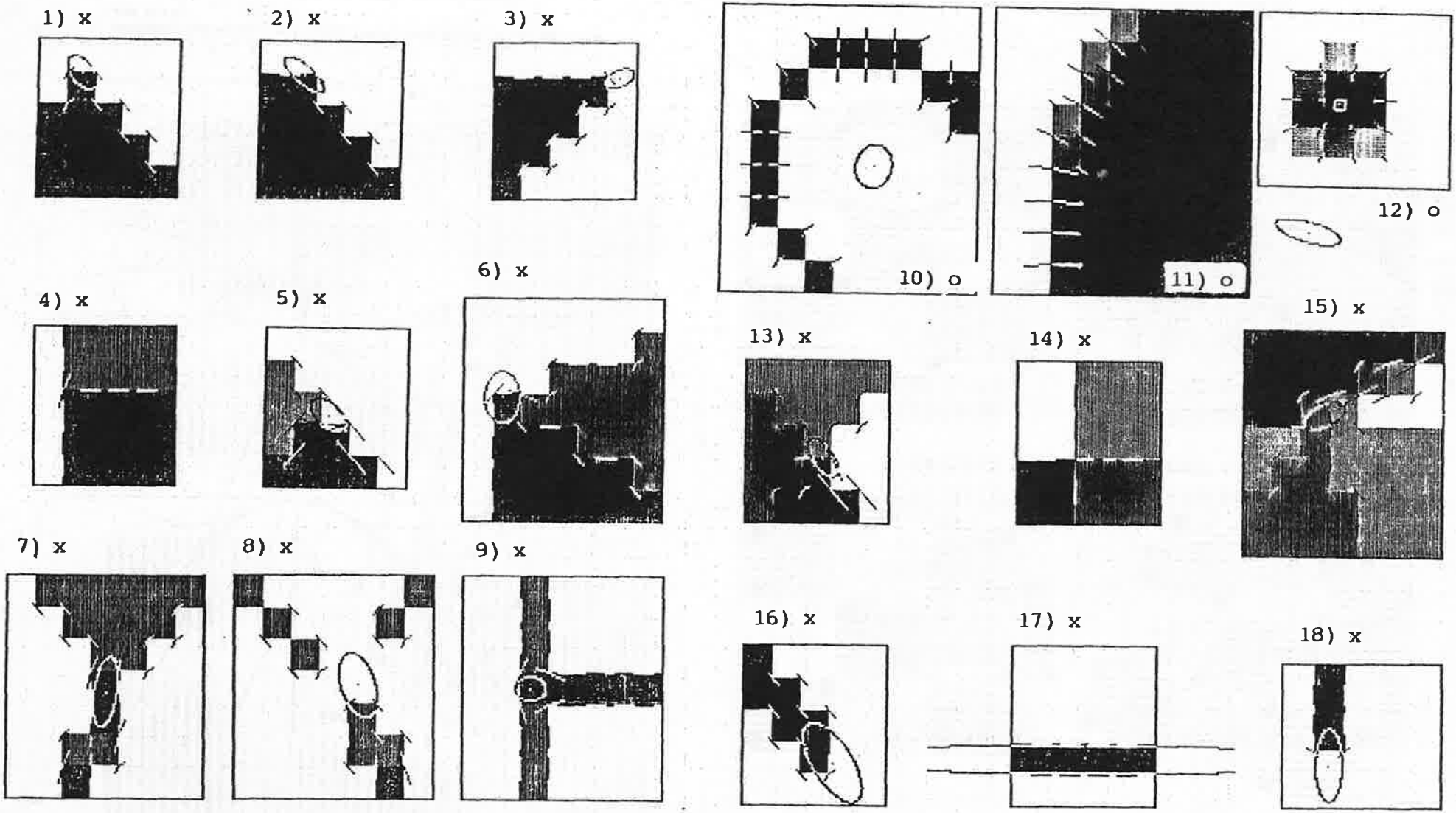

Fig. 5 Result of point selector (sect. 4.2) based on different selected windows
Simulated data
edge-elements for intersection-, corner-points (x)
slope elements for centers of circles and discs (o)
99 %-confidence ellipse estimated from fit of gray levels to model

International Society for
Photogrammetry and Remote Sensing

Commission III

International Archives of Photogrammetry
and Remote Sensing

Volume 26 Part 3/3

Proceedings of the Symposium

FROM ANALYTICAL TO DIGITAL

Edited by E. KILPELÄ
A. SAVOLAINEN
A. LAIHO

August 19-22, 1986

Lappia-House
Rovaniemi, Finland

TOC

ISSN 0256-1840

Technische Informationsbibliothek (TIB)
German National Library of Science and Technology

Technische
Informationsbibliothek (TIB)
German National Library of
Science and Technology
Welfengarten 1 B
30167 Hannover, Germany
T +49 511 762-8989
F +49 511 762-8998
customerservice@tib.eu
www.tib.eu

Hannover,10.11.2016

Hoegskolebiblioteket i Halmstad

Box 823
301 18 Halmstad
Schweden

SUBITO - document delivery - delivery note (please wait for invoice)

delivery notifications

customer number:	SLI02X00444E
order number:	SUBITO:2016110901328
order date:	09.11.2016
delivery service	FTP
delivery type:	copy
delivery priority:	normal

customer data:

name:	Ms Anna Matovic
E-Mail:	bibflan@hh.se
reference number:	

bibliographic reference:

shelf mark:	ZS 312 [Haus2]
title:	International archives of photogrammetry and remote sensing
volume/issue:	3(26)
date of publication:	
pages:	150-166
author:	Wolfgang Foerstner
article:	A feature based correspondence algorithm for image matching